



Immobilisation of CdS nanoparticles on chitosan microspheres via a photochemical method with enhanced photocatalytic activity in the decolourisation of methyl orange

Lihe Zhang^a, Fengqiang Sun^{a,b,c,*}, Yanbing Zuo^a, Caifeng Fan^a, Shipu Xu^a, Shumin Yang^a, Fenglong Gu^b

^a School of Chemistry and Environment, South China Normal University, Guangzhou 510006, PR China

^b Key Laboratory of Theoretical Chemistry of Environment, Ministry of Education, South China Normal University, PR China

^c Exhibition Base of Production, Study & Research on New Polymer Materials and Postgraduate Students' Innovation Training of Guangdong Higher Education Institutes, PR China

ARTICLE INFO

Article history:

Received 6 October 2013

Received in revised form 1 March 2014

Accepted 10 March 2014

Available online 18 March 2014

Keywords:

CdS

Chitosan microsphere

Photochemical method

Photocatalytic activity

Methyl orange

ABSTRACT

In this study, CdS nanoparticles were directly grown on the surfaces of chitosan microspheres (CM) via photochemical method with irradiation from an 8 W ultraviolet (UV) lamp. The nanoparticles exhibited an almost spherical shape, were closely arranged, and were immobilised on the microspheres because of the induction of the amino and hydroxyl groups of the chitosan. The CM-immobilised CdS nanoparticles showed higher activity and easier recyclability than pure CdS particles obtained in the same conditions when used in the decolourisation of methyl orange (MO) under UV–vis light. The experiments proved that the photodegradation of MO was mainly caused by the oxidation of superoxide radicals ($\cdot\text{O}_2^-$) generated by the reaction between the electrons and the adsorbed O_2 . The functional groups of CM may prevent the recombination of electron/holes and effectively promote photocatalytic reactions. This photochemical method is new, general, and promising for the immobilisation of catalyst particles on polymer microspheres, which results in enhanced activity.

© 2014 Elsevier B.V. All rights reserved.

1. Introduction

CdS is a well-known semiconductor with a band gap of 2.42 eV, and its valence electron can be easily evoked to the conduction band when the wavelength of the evoking light is <495 nm [1]. Therefore, many nanostructured CdS-based materials have been used in the photocatalytic removal of dyes in waste water because of their unique photochemical and photophysical properties. These materials include Cd-doped CdS nanotubes [2], Ni-doped CdS hollow microspheres [3], and several CdS-sensitised semiconductors [4–8]. Pure CdS nanostructures also have the excellent properties [9,10]. However, far fewer studies [11,12] have reported on the direct applications of pure CdS nanoparticles in photocatalysis, especially in the photodegradation of pollutants in solutions because of three possible reasons. First, CdS nanoparticles easily aggregate

in aqueous solution, which results in decreased efficiency. Second, as a powdery catalyst, CdS particles are difficult to recycle and reuse. Third, the suspended particles are difficult to remove, thereby resulting in secondary pollution. An effective method to overcome these defects is to load these nanoparticles into polymer matrixes [13–16]. However, in these composites, many CdS nanoparticles are inevitably sealed in the matrix, and only partial particles on the surface can exhibit their activities under light irradiation. Thus, the photodegradation efficiency decreases. The immobilisation of CdS nanoparticles onto the surface of a suitable polymer with a regular morphology is thus necessary to enhance the photocatalytic activities.

Chitosan is a natural, abundant, environment-friendly, and active biopolymer that possesses good chelating ability with transition metal ions. This biopolymer can be used as an excellent matrix for the preparation of heterogeneous photocatalysts, such as TiO_2 -chitosan beads [17], ZnO/SnO_2 -chitosan film [18], Cu_2O -chitosan film [19], Nb_2O_5 -chitosan film [20], and chitosan/nano-CdS powder [21]. To obtain these composites, chitosan raw materials are first dissolved, mixed with semiconductor nanoparticles, and finally crosslinked with chitosan chains to wrap the nanoparticles.

* Corresponding author at: School of Chemistry and Environment, South China Normal University, Guangzhou 510006, PR China. Tel.: +86 20 39310187; fax: +86 20 39310187.

E-mail address: fqsun@scnu.edu.cn (F. Sun).

However, immobilising the semiconductor nanoparticles only on the surface of the crosslinked chitosan is impossible. The embedded semiconductor nanoparticles do not contribute to the photocatalytic activities and increases the difficulties for the crosslink polymerisation of chitosan. Thus, the introduction of these nanoparticles becomes unnecessary. Studies on the photocatalytic mechanisms of the composites have shown that the adsorption ability of chitosan enhances the activity of a semiconductor, and hydroxyl radicals have been considered as the main oxidants for the decomposition of pollutant molecules. However, these findings are limited in theoretical analyses because direct experimental proofs are lacking.

Microspheres have smooth homogeneous surfaces, can be easily recollected, and should be used as ideal supports to load semiconductor nanoparticles. However, achieving these features still remains a challenge for the fabrication of chitosan microspheres (CM) to date. In this study, we introduce a simple photochemical method to prepare CdS directly on CM. CMs were first prepared via crosslink polymerisation and were then dispersed into a specific precursor aqueous solution. The CdS particles can be directly formed and stabilised on the microspheres under UV light irradiation at room temperature. The as-prepared CdS-chitosan composite microspheres obey a new chitosan-involved oxidation mechanism and show highly enhanced photocatalytic activities in the photodegradation of methyl orange (MO) under UV-vis light. The method is green, low-cost, and easily to carry out in the fabrication of semiconductor nanoparticles on polymers.

2. Experimental details

2.1. Preparation of CM

Approximately 0.15 g of chitosan was completely dissolved into 15 mL of 1% (v/v) aqueous acetic acid in a flask. Subsequently, 75 mL of paraffin liquid containing 8% span-80 was added into the solution to form an emulsion system. The emulsion system was first mechanically agitated for 30 min at 1500 rpm and then vigorously stirred in a 60 °C water bath until the water phase was uniformly dispersed. Approximately 2 mL of 25% glutaraldehyde was used as a pre-crosslinking agent and was slowly added into the suspension. After stirring for 60 min at 1500 rpm, 2 mL of 25% glutaraldehyde was again added to the system, which was then continuously stirred for additional 2 h. The resulting products were collected via centrifugation, washed with petroleum ether and acetone to remove the unreacted chitosan and other impurities, and then dried at 50 °C.

2.2. Preparation of CdS nanoparticles on CM

In a typical synthesis, 100 mL of mixed solution of CdSO₄ (0.05 M) and Na₂S₂O₃ (0.30 M) in a beaker was used as the precursor. Approximately 0.05 g of CM was added into the solution, and the beaker was then placed in an ultrasonic bath for a few minutes to disperse the microspheres thoroughly in the solution. Subsequently, the beaker was placed under a tube-type UV lamp (Philips, 245 nm, 8 W, and 0.734 mW cm⁻²) in a box, and the suspension was constantly stirred. After being irradiated for 24 h, yellow particles were formed. The particles were then collected using a centrifugal separator, sequentially washed 3–5 times with deionised water, trichloroethylene (to remove sulphur), ethanol, 0.1 M dilute nitric acid (to remove metallic cadmium) and deionised water, respectively. Finally, the sample was dried at 50 °C in atmospheric condition. To calculate the CdS content in the composite, a given weight of composite was weighed with an analytic balance, dissolved with diluted hydrochloric acid, and then measured

the concentration of Cd²⁺ with an Atomic Absorption Spectrophotometer (TAS-986) to further calculate the weight of CdS.

2.3. Decolourisation experiments

The decolourisation of MO was carried out in an aqueous solution at an ambient temperature. About 0.05 g of CdS-chitosan composite microspheres was dispersed in 200 mL of 8×10^{-5} mol L⁻¹ MO solution, and the mixture was then placed in a column-like container (60 mm diameter, 300 mm height) with a magnetic stirrer. The samples were then regularly taken out from the reactor and immediately centrifuged to separate any suspended solid. The transparent solution was analysed using a UV-vis spectrometer, and the absorbance was measured at a wavelength of 464 nm, which corresponds to the maximum absorption wavelength of MO. To record the real photocatalytic activity of the catalyst, the measured solution and the centrifuged particles were poured back into the original glass to maintain a consistent total amount of MO in the solution.

3. Results and discussion

3.1. Morphologies and growth mechanism of CdS nanoparticles on CM

Fig. 1a shows the SEM image of the obtained CM. A single microsphere has a well-defined spherical shape and smooth surface. The sizes of the microspheres were in the range of 80–800 nm. The Brunauer–Emmett–Teller (BET) specific surface area of these CM was measured as 29.1 m² g⁻¹ (nitrogen adsorption–desorption isotherm was not shown here). The FT-IR spectra of the microspheres and the chitosan reagent are shown in Fig. 1b. Compared with those of the pure chitosan reagent, the characteristics of the molecular structure of the microspheres were not changed during the preparation process. The peaks at around 3400, 1650 and 1597 cm⁻¹ are attributed to the hydroxyl group (–OH), amide I and amide II [22], respectively, which are typical features of chitosan. Chitosan has a good chelating ability with transition metal ions because of the presence of these groups [23]. Thus, metal ion complexes of chitosan can be used as precursors for synthesising CdS composites [24]. The spherical shape could not change the inherent properties of the chemical groups.

These CMs can induce the growth of CdS nanoparticles in CdSO₄ and Na₂S₂O₃ mixed solution under the irradiation of UV light. Fig. 2a shows the XRD pattern of the product obtained from the solution after being irradiated for 24 h. Three characteristic peaks appeared at 26.53°, 43.95°, and 52.12°, which correspond to the (1 1 1), (2 1 0), and (3 1 1) crystal faces of CdS (JCPDS no.75-1546), respectively. The content of CdS in the composite was calculated as ~58.1 wt%. The SEM image of the product (Fig. 2b) shows that CdS nanoparticles were formed, immobilised, and closely arranged on the surface of the CM (CM-immobilised CdS nanoparticles is defined as CM/CdS in this study). Nearly no nanoparticle was separated from the CM. Most nanoparticles exhibited a nearly spherical shape with a size of ~80 nm. Many CM/CdS composite particles aggregated together, but this phenomenon should be the result of CM aggregation before the formation of CdS nanoparticles. Correspondingly, the composite displayed a BET specific surface area of 5.6 m² g⁻¹, lower than that of pure CM. Nevertheless, CdS nanoparticles always grew on the surface of CM independently, could not be buried, and could not aggregate. Every CdS nanoparticle can be discerned, and most of the surface is exposed. In the control experiment, pure CdS nanoparticles (Fig. 2c) could also be formed under the same light source and had similar sizes with those immobilised on CM when no chitosan microsphere was dispersed in the

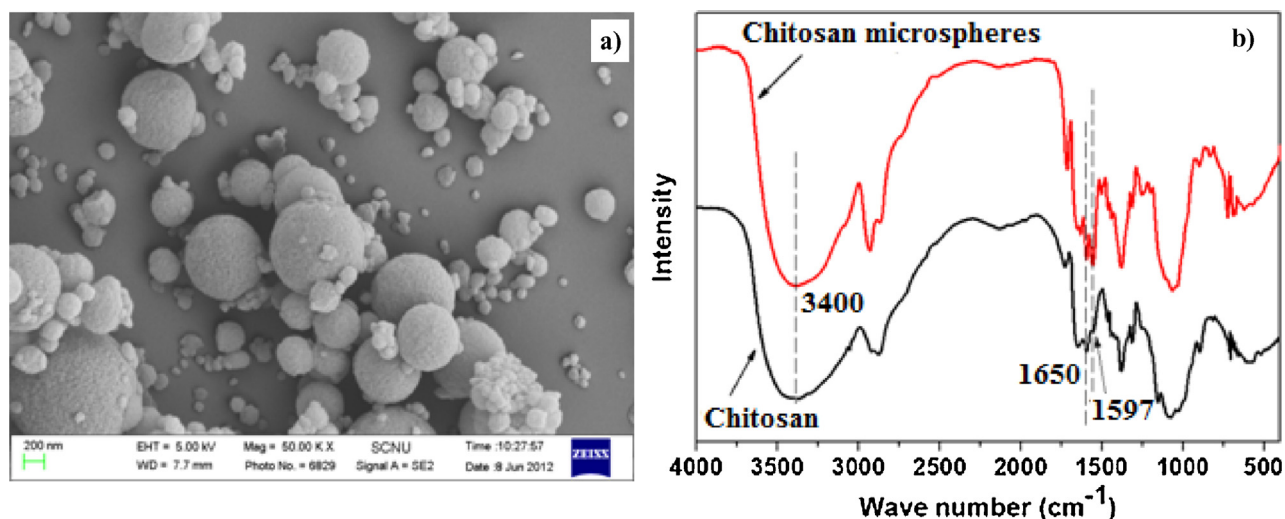


Fig. 1. SEM image (a) and FTIR spectra (b) of the chitosan microspheres.

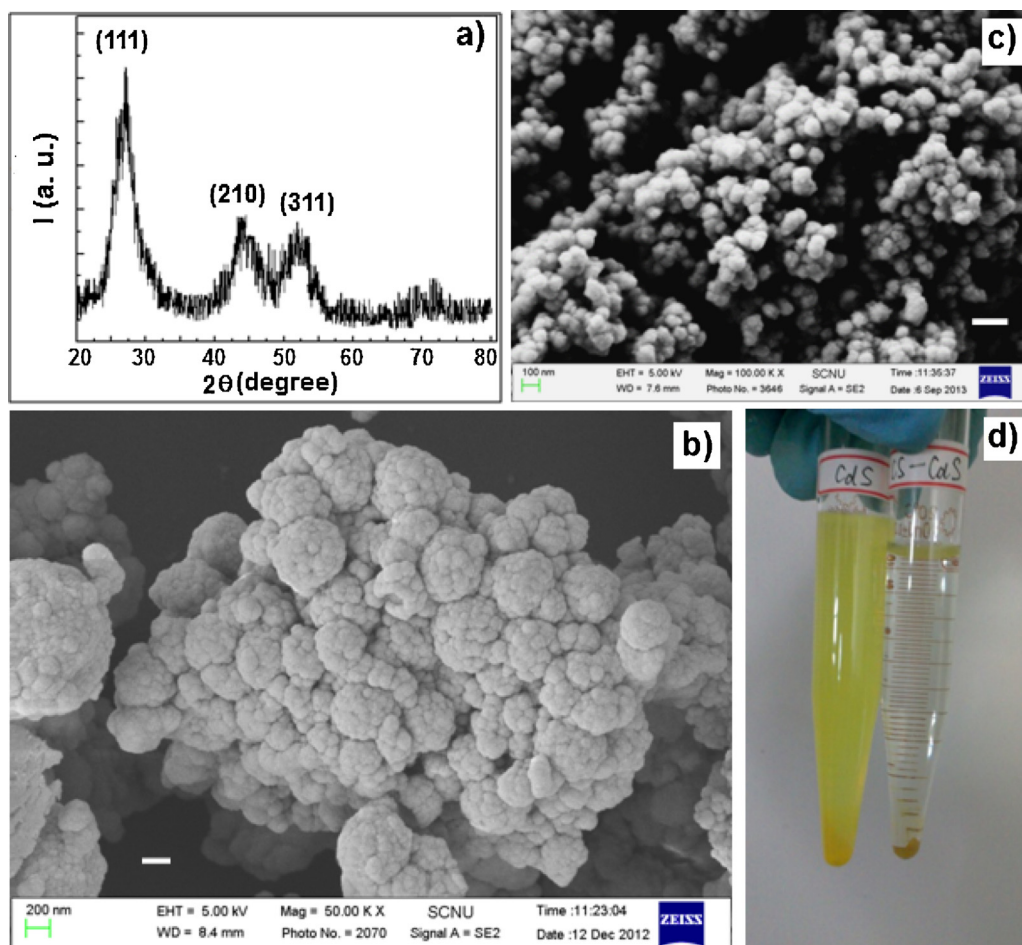


Fig. 2. Characterisations of CM/CdS and pure CdS nanoparticles. (a) XRD pattern of CM/CdS; (b) SEM image of CM/CdS; (c) SEM image of pure CdS nanoparticles obtained in the same conditions (scale bar = 200 nm); and (d) photos of CM/CdS and pure CdS nanoparticles in centrifuge tubes after centrifugally separated in the same rate of 2500 r/min.

precursor solution. The sample showed a higher BET specific surface area than CM/CdS, $11.6 \text{ m}^2 \text{ g}^{-1}$. However, many discernible nanoparticles aggregated because of their high surface energy, which resulted in a decrease in the total exposed surface. More disadvantageously, such nanoparticles could not be fully re-collected when used in solutions compared with CM/CdS. To prove this

finding, the same amounts of CM/CdS and pure CdS nanoparticles were dispersed in deionised water, as shown in Fig. 2d. After centrifugation in the same conditions, all CM/CdS particles settled at the bottom of the centrifugal tube, whereas many fine particles were still suspended in the water in the tube containing the pure CdS sample.

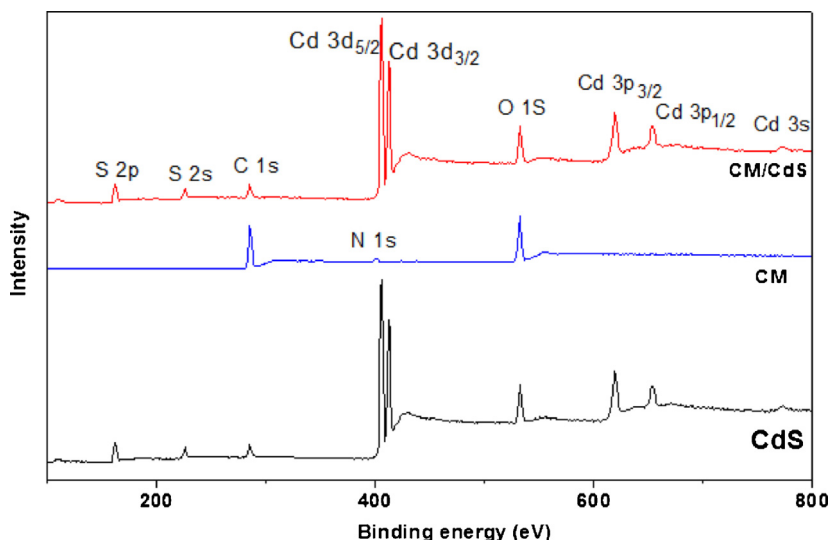
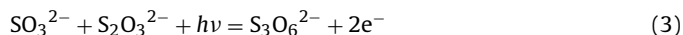


Fig. 3. XPS survey spectra of CM/CdS, CM and the pure CdS nanoparticles.

Fig. 3 shows the XPS survey spectra of CM, CM/CdS and the pure CdS nanoparticles. It is clear that only Cd, S, C and O elements are observed in both CM/CdS and pure CdS samples; only C, N and O elements are detected in CM. The binding energy of every detected element in CM/CdS is same as that of in the pure CdS samples. This explains the CdS on the CM and the pure CdS particles have the same chemical composition, there is no chemical interaction between the as-formed CdS nanoparticles and CM, and there is no Cd^{2+} adsorbed on the surface of CM. The binding energies of S $2p_{3/2}$, S $2p_{1/2}$, Cd $3d_{3/2}$ and Cd $3d_{5/2}$ are identified at 161.6 eV, 162.8 eV, 412.3 eV and 405.5 eV, respectively, which is consistent with the previous reported values for CdS [25–27]. The Cd $3d_{5/2}$ and S $2p_{3/2}$ peak areas were determined for the quantitative elemental analysis of Cd and S in the products, and an atomic ratio of approximately 1:1 has been obtained. The carbon element should mainly come from the adsorbed CO_2 and the oxygen element came from the adsorbed molecular O_2 or H_2O . Compared with the spectrum of the CM sample, no N 1s peak can be discerned and the intensity of C 1s is obviously decreased in the CM/CdS sample, explaining the CdS nanoparticles have covered almost the whole surface of CM in the composite.

The formation of CdS nanoparticles on CM was suggested as follows: when CM (Scheme 1a) were dispersed into the precursor solution composed of $\text{Na}_2\text{S}_2\text{O}_3$ and CdSO_4 , part of Cd^{2+} can be adsorbed and immobilised on the surface because of the coordination that occurred between Cd^{2+} and the functional groups ($-\text{OH}$ and $-\text{NH}_2$) of chitosan (Scheme 1b). When irradiated with UV light, the $\text{S}_2\text{O}_3^{2-}$ ions in the solution dissociated into sulphur and some sulphur-containing complex ions (Eqs. (1)–(3)) [2,28]. Moreover, solvated electrons were also generated. Based on the general nucleation theory, the hydrophilic solid surface and the aqueous solution can form a low-energy interface for the easy formation of crystal nuclei. In this study, the adsorbed Cd^{2+} can also increase the heterogenic compatibility between CM and the CdS solid to be formed. Therefore, the generated sulphur and electrons would preferentially combine with Cd^{2+} on the surface of CM to form CdS nuclei (Scheme 1c). CdS nuclei could be adsorbed on the surface of CM via the Van de Waals Force. Subsequently, the CdS crystal nuclei adsorbed the corresponding ions in the solution and gradually grew with continuous irradiation of UV light (Scheme 1d) [29]. With the assistance of magnetic agitation, every site on the surface of CM can be exposed to light irradiation with the same intensity. Hence, CdS nanoparticles homogeneously grew on the surface

of CM and formed into spherical shapes.



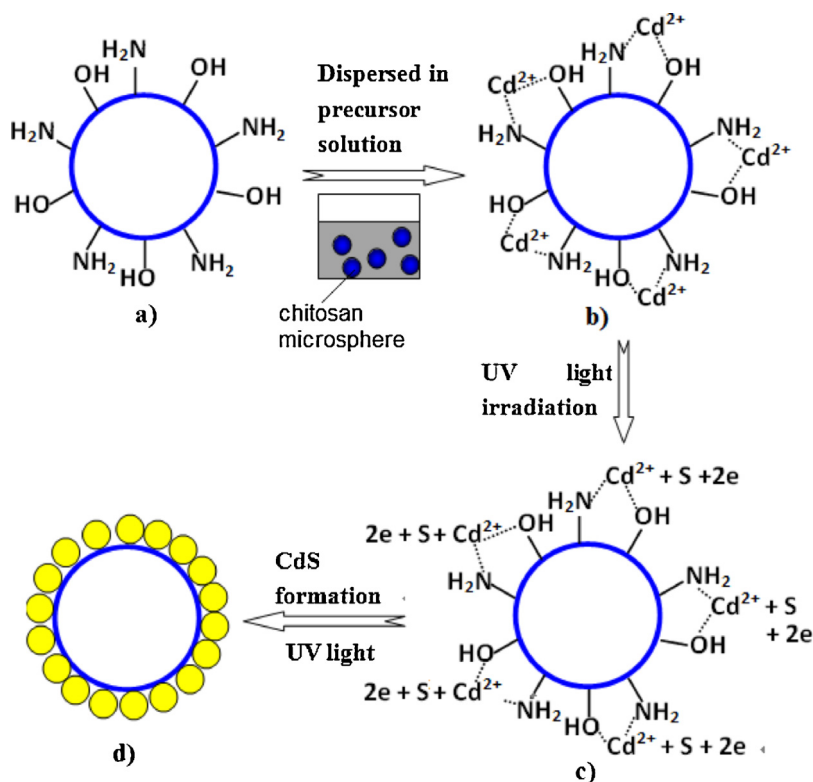
3.2. Decolourisation process of MO in the presence of CM/CdS

CM/CdS exhibited excellent performances in the decolourisation of MO, as shown in Fig. 4. The decolourisation experiments are divided into two stages, i.e., 30 min adsorption stage and 70 min photodegradation stage (Fig. 4a). Without any catalyst, the decolourisation efficiency of MO only reached 20.9% in 100 min because of photodegradation under UV light. When pure CdS particles (shown in Fig. 2c) were used, the efficiency slightly increased and reached 34.1%, which constitute 7.8% adsorption and 26.3% photodegradation decolourisation. This finding indicates that the CdS prepared via photochemical method possessed both low adsorption ability and low photocatalytic activity. In the presence of CM/CdS, a decolourisation efficiency of 22.4% was observed in the first 30 min because of adsorption; the chemical oxygen demand (COD) decreased 15.0% (inset in Fig. 4a). When the MO solution was continuously placed in the dark, the efficiency only increased to 30.1%. Therefore, the adsorption in 30 min nearly reached equilibrium, and the MO solution can be completely decolourised depending on the adsorption ability of the particles. Alternatively, under light irradiation, MO decolourisation could reach to 95.2% and the COD decreased 71.6% in 70 min, which indicated that CdS/CM had a higher photocatalytic activity than pure CdS particles. However, the CdS nanoparticles on CM and the pure CdS had similar sizes (shown in Fig. 2b and c) and the actual quantity of CdS in the composite was only near half of that of the pure.

The photodegradation reactions (in the second stage of decolourisation) of MO in the presence of CM/CdS or pure CdS particles exhibited a modified pseudo-first-order kinetic model with respect to irradiation time. The results are nearly consistent with the linear equation [30]:

$$\ln \frac{C_0}{C} = kt \quad (4)$$

where C_0 is the initial concentration of a pollutant, C is the concentration of a pollutant at time t , and k is the reaction constant of the



Scheme 1. Schematic of the formation process of CdS nanoparticles on chitosan microspheres: (a) chitosan microsphere and its functional groups; (b) Cd^{2+} are adsorbed on the microsphere; (c) reactions between Cd^{2+} and sulphur under UV light; and (d) CdS nanoparticles on microspheres.

first-order reaction. A linear relationship can always be obtained with more than 98% linear fit (R^2), which indicates excellent agreement with the given model, as shown in Fig. 4b. The reaction rate constants showed that the activity of CM/CdS increased more than 6.8 times compared with that of pure CdS particles.

The loss of CdS was effectively reduced when re-collected via centrifugation because CdS nanoparticles were immobilised onto CM and the composite size was much larger than that of any single CdS nanoparticle. This characteristic caused the catalyst to be easily recycled, which is an important parameter of the photocatalytic process because a long period of time results in a significant cost reduction of the treatment. The decolourisation experiments were repeated five times with the same catalyst (Fig. 5a). The decolourisation ratios for the five cycling reuses were 95.2%, 91.6%, 91.2%, 84.8%, and 84.3% in 100 min. Except for the first usage, the decolourisation by adsorption only reached to $\sim 2\%$ in 30 min from the 2nd to the 5th usage. The reusability is attributed to the high photocatalytic activities of CdS nanoparticles immobilised on CMs.

The pseudo-first-order kinetic model of every photodegradation reaction in every usage is summarised in Fig. 5b to evaluate the activity of the catalyst during its reuse. According to the reaction rate constants, the activity showed a small decrease compared with the former usage. The decrease is attributed to a small loss of catalyst during washing and the inevitable photocorrosion of CdS [31,32]. Nevertheless, the activity of CdS nanoparticles was still higher than 4.0 times that of pure CdS powder after five usages.

3.3. Effects on the decolourisation

Further experiments show that the decolourisation was closely related to the irradiation time during the preparation of CdS nanoparticles (Fig. 6a). All products obtained within 6–24 h can induce a nearly complete decolourisation of MO in 100 min. However, the adsorption for MO gradually increased within 30 min with decreasing irradiation time, which indicates that the produced CdS nanoparticles were too small on the CM. Moreover, the CM

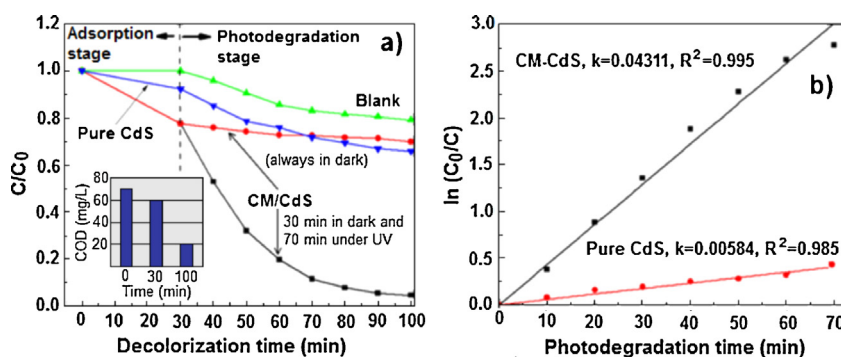


Fig. 4. (a) Decolourisation of MO in the presence of CM/CdS or pure CdS particles with or without irradiation of UV light; the inset shows the variation of COD. (b) The first-order kinetics photodegradation of MO in the presence of different catalysts.

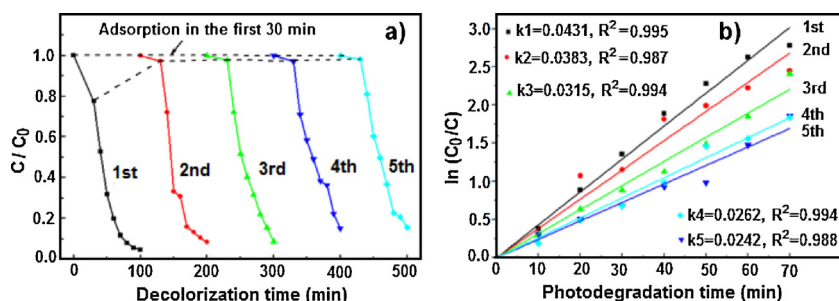


Fig. 5. Reuse of CM/CdS nanoparticles. (a) Catalyst recycling in the decolourisation of MO and (b) the first-order kinetics in the photodegradation of MO solution during the reuse of the catalyst.

surface was further exposed, thereby facilitating MO absorption when the irradiation time was too short (6–18 h). In 30 min, the adsorption cannot reach the saturation point, and the adsorption still occurred even in the photo-induced decolourisation process. When the MO molecules were adsorbed onto the CM, they were not easily removed, which was disadvantageous for the reuse of the catalyst. Therefore, the product obtained via irradiation for 24 h was optimised to be used as a stable and recyclable catalyst in the decolourisation of MO. When the irradiation time was continuously increased, the performance of the products was only slightly improved, but the preparation period was prolonged. Thus, this step of the process was unnecessary.

The dose of CM/CdS would also affect the adsorption, the photodegradation and the final decolourisation efficiency (Fig. 6b). Easily understood, with the increase of the dose, the adsorbed MO molecules gradually increased. For the photodegradation, when the dose was lower than 0.02 g (i.e., the concentration of the catalyst was lower than 0.1 g L^{-1}) the photodegradation efficiency was obviously low because the employed catalyst could not provide enough active sites. When the dose was increased to 0.05–0.08 g, the photodegradation efficiency was improved a lot. However, in the range, the efficiency was changed a little with the increase of the catalyst dose and the same efficiencies could be obtained in 100 min independent of the dose employed. In practical application, the smaller quantity (0.05 g) of catalyst should be optimised. Additionally, the initial concentration of MO would put impact on the decolourisation rate. With increase of the concentration, the rate gradually decreased (Fig. 6c). Nevertheless, the as-prepared CM/CdS catalyst had high ability in decolourisation of MO, and $2.0\text{--}10.0 \times 10^{-5} \text{ mol L}^{-1}$ MO could be nearly completely decolourised in proper time. According to this trend, a higher concentration of the MO solution would be efficiently degraded.

3.4. Decolourisation mechanism

The adsorption decolourisation was mainly caused by the residual $-\text{NH}_2$ and $-\text{OH}$ groups on CM. These groups can combine with the sulphonic acid groups ($-\text{SO}_3$) of the MO molecule [33]. When CM/CdS particles were immersed into the MO solution, some MO molecules diffused through the cracks among the CdS nanoparticles and reached the surface of CM where they were adsorbed. In 30 min, the adsorption could almost reach the saturation point, and the adsorbed MO molecular cannot be removed any more. Thus, decolourisation efficiency by adsorption was not changed since the second usage of the catalyst.

The photocatalytic decomposition of MO molecules by CdS nanoparticles is the main factor that causes decolourisation. Based on the reuse characteristic of CM/CdS (Fig. 5), the adsorption of CM can promote the total decolourisation of MO but cannot increase the photocatalytic activity of CdS nanoparticles. Therefore, the increased exposed surfaces of the CdS nanoparticles caused by immobilisation might improve the activity compared with pure CdS and the groups ($-\text{OH}$ and $-\text{NH}_2$) of CM.

In many reports, super oxide ions ($\cdot\text{O}_2^-$), hydroxyl radicals ($\cdot\text{OH}$) and holes could oxidise and decompose the MO molecules in the solution [34,35]. To determine the photocatalytic degradation mechanism, a hydroxyl radical scavenger (*t*-butanol) and a hole scavenger (methanol) were added into the MO solution in the control experiments. However, both increased the photodegradation rate (Fig. 7) regardless of the amount of the additions. Moreover, with the increase of the amount of the scavengers, the photodegradation rate increased. These findings suggested that the free hydroxyl radicals and the holes were not the main active oxidative species in the photocatalytic degradation of MO. Alternatively, pure nitrogen (N_2) was bubbled through the MO solution to exclude the adsorbed and dissolved oxygen during the photodegradation

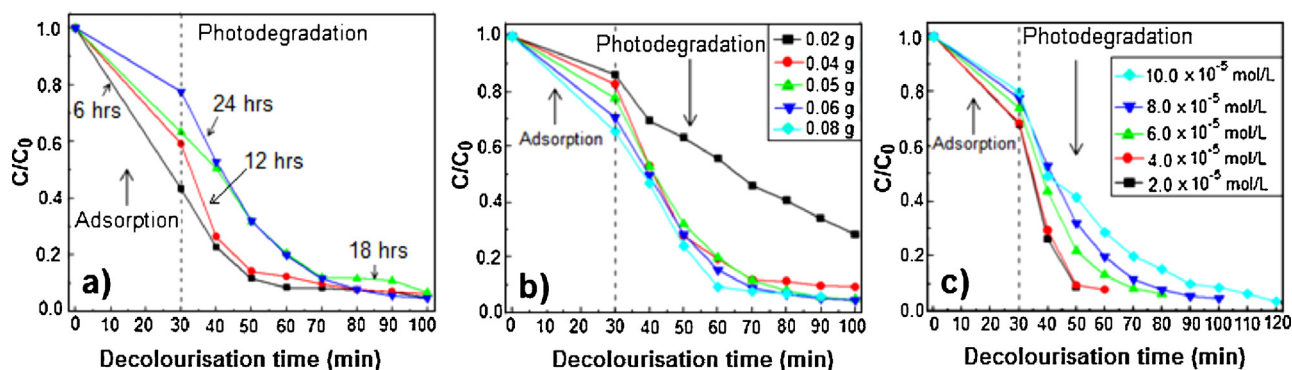


Fig. 6. Effects on the decolourisation of MO solution. (a) Effect of irradiation time during the preparation of CM/CdS; (b) effect of the dose of CM/CdS; and (c) effect of the initial concentration of MO.

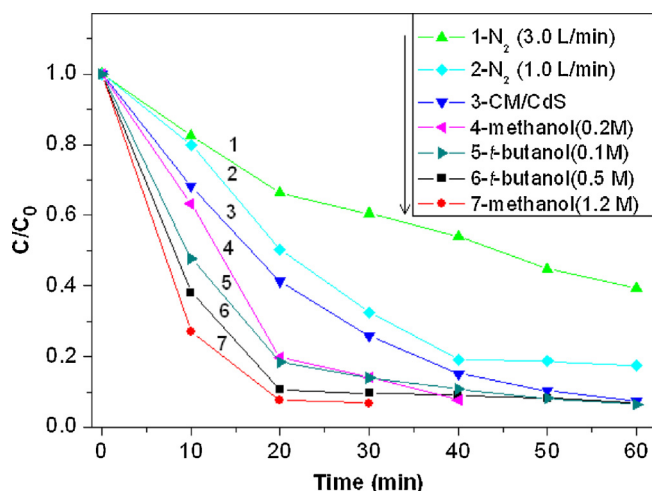


Fig. 7. Photodegradation of the same concentration of MO solution by using CM/CdS added with *t*-butanol and methanol or bubbled with N_2 at different flow rates.

process [36]. Surprisingly, the photodegradation rate was significantly decreased, and the decrease was related to the gas flow rate. A high flow rate indicates a low degradation rate of the MO. The oxygen molecules in the solution had crucial effects on the photodegradation of MO. Therefore, the main photocatalytic process can be suggested, as shown in Scheme 2. When CdS nanoparticles were irradiated with UV light, the electrons of the valence bands (VB) are excited to the conductor bands (CB) (Eq. (5)). Thus, positive holes (h^+) are produced in the VB. The electrons then react with the O_2 molecules adsorbed on the surface of CdS to generate super oxide ions ($\bullet O_2^-$) [37] (Eq. (6)). Subsequently, the MO molecules are oxidised by $\bullet O_2^-$ ions and decomposed into inorganic or nontoxic material (Eq. (7)). The nanoparticles came into contact with these surface groups of CM at the molecular level and the electron structure of $-NH_2$ and $-OH$ had important effects on the photocatalytic process because the nanoparticles directly grew on the surface of CM under the induction of the $-NH_2$ or $-OH$ groups. A synergy effect may exist between these groups and the CdS nanoparticles. Lone pair electrons of these groups can draw the photogenerated holes and repel excited electrons, which lowers the electron–hole recombination rate. The electrons were effectively

utilised to produce more $\bullet O_2^-$, and the photodegradation rate was thereby increased.



During the production of $\bullet O_2^-$ and holes, some holes could still oxidise H_2O molecules to generate $\bullet OH$ (Eq. (8)) [38]. However, because of the attractions of the electrons in the $-NH_2$ or $-OH$ groups of CM, the available holes were limited, leading to fewer $\bullet OH$ produced. As a result, only a small quantity of MO molecules could be directly decomposed by the holes and $\bullet OH$ in the solution. When *t*-butanol was added into the solution, it could consume the $\bullet OH$, and according to Eq. (8), the amount of holes would be decreased, further decreasing the chance of recombination between electrons and holes. Correspondingly, more photogenerated electrons could be employed to generate more $\bullet O_2^-$ and the decomposition of MO via the $\bullet O_2^-$ was enhanced. The increased amount of MO decomposed by $\bullet O_2^-$ was larger than the decreased amount caused by the decrease of $\bullet OH$ quantity, resulting in the improved final photodegradation rate (Fig. 7). For the same reason, the hole scavenger could also increase the degradation rate.



4. Conclusions

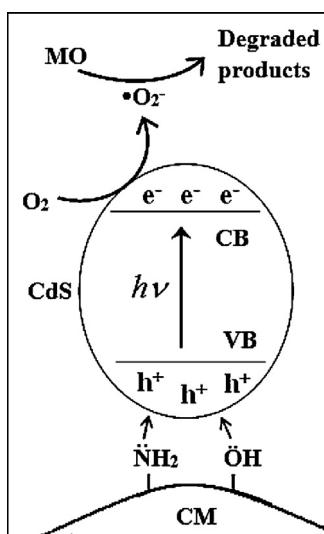
CdS nanoparticles were prepared and immobilised on the surface of CM via room-temperature photochemical route under the irradiation of a low-power UV lamp. Compared with the pure CdS particles obtained in the same conditions, the as-prepared CM/CdS particles exhibited a much higher photocatalytic activities and easier recyclability in the decolourisation of MO. The immobilisation and the $-NH_2$ and $-OH$ groups on the surface of CM may have caused the enhancement in photocatalytic activities. The superoxide radical oxidation pathway in the photocatalytic process is new for CdS serial photocatalysts and chitosan involved composite photocatalysts. Further works that hybridise CM with other photocatalysts are underway.

Acknowledgements

This work was co-supported by the National Natural Science Foundation of China (No. 31071057), the Research Project of Chinese Ministry of Education (No. 213029A) and the Natural Science Foundation of Guangdong Province (Nos. 10351063101000001 and S2011010003499).

References

- [1] J.S. Jie, W.J. Zhang, Y. Jiang, X.M. Meng, Y.Q. Li, S.T. Lee, *Nano Lett.* 6 (2006) 1887–1892.
- [2] Y.Y. Huang, F.Q. Sun, H.J. Wang, Y. He, L.S. Li, Z.X. Huang, Q.S. Wu, J.C. Yu, J. Mater. Chem. 19 (2009) 6901–6906.
- [3] M. Luo, Y. Liu, J.C. Hu, H. Liu, J.L. Li, *ACS Appl. Mater. Interfaces* 4 (2012) 1813–1821.
- [4] J.C. Yu, L. Wu, J. Lin, P.S. Li, Q. Li, *Chem. Commun.* (2003) 1552–1553.
- [5] Y. Hu, X.H. Gao, L. Yu, Y.R. Wang, J.Q. Ning, S.J. Xu, X.W. Lou, *Angew. Chem. Int. Ed.* 125 (2013) 5746–5749.
- [6] X.L. Mao, D.X. Xu, M.L. Fu, B.L. Yuan, J.W. Shi, H.J. Cui, *Chem. Eng. J.* 218 (2013) 73–80.
- [7] X.B. Liu, D.R. Sun, R.S. Yuan, X.Z. Fu, Z.H. Li, *J. Catal.* 304 (2013) 1–6.
- [8] L.J. Shen, S.J. Liang, W.M. Wu, R.W. Liang, L. Wu, *J. Mater. Chem. A* 1 (2013) 11473–11482.
- [9] D.W. Jing, L.J. Guo, *J. Phys. Chem. B* 110 (2006) 11139–11145.
- [10] Q.J. Xiang, B. Cheng, J.G. Yu, *Appl. Catal. B – Environ.* 138–139 (2013) 299–303.
- [11] H.B. Yin, Y.J. Wada, T. Kitamura, S. Yanagida, *Environ. Sci. Technol.* 35 (2001) 227–231.
- [12] A. Datta, A. Priyam, S.N. Bhattacharyya, K.K. Mukherjee, A. Saha, *J. Colloid Interface Sci.* 322 (2008) 128–135.



Scheme 2. Schematic of the photodegradation process of MO by CM/CdS.

- [13] T. Hirai, M. Miyamoto, T. Watanabe, S. Shiojiri, I. Komasaawa, J. Chem. Eng. Jpn. 31 (1998) 1003–1006.
- [14] B.C. Pan, Y.M. Xie, S.J. Zhang, L. Lv, W.M. Zhang, ACS Appl. Mater. Interfaces 4 (2012) 3938–3943.
- [15] Y.M. Xie, S.J. Zhang, B.C. Pan, L. Lv, W.M. Zhang, Chem. Eng. J. 174 (2011) 351–356.
- [16] R. Jiang, H.Y. Zhu, J. Yao, Y.Q. Fu, Y.J. Guan, Appl. Surf. Sci. 258 (2012) 3513–3518.
- [17] T.Y. Kim, Y.H. Lee, K.H. Park, S.J. Kim, S.Y. Cho, Res. Chem. Intermediat. 31 (2005) 343–358.
- [18] H.Y. Zhu, L. Xiao, R. Jiang, G.M. Zeng, L. Liu, Chem. Eng. J. 172 (2011) 746–753.
- [19] J.Y. Chen, P.J. Zhou, J.L. Li, Y. Wang, Carbohydr. Polym. 72 (2008) 128–132.
- [20] J.D. Torres, E.A. Faria, J.R. SouzaDe, A.G.S. Prado, J. Photochem. Photobiol. A – Chem. 182 (2006) 202–206.
- [21] H.Y. Zhu, R. Jiang, L. Xiao, Y.H. Chang, Y.J. Guan, X.D. Li, G.M. Zeng, J. Hazard. Mater. 169 (2009) 933–940.
- [22] X.H. Wang, D.P. Li, W.J. Wang, Q.L. Feng, F.Z. Cui, Y.X. Xu, X.H. Song, M. van der Werf, Biomaterials 24 (2003) 3213–3220.
- [23] E. Guibal, Prog. Polym. Sci. 30 (2005) 71–109.
- [24] B. Krajewska, React. Funct. Polym. 47 (2001) 37–47.
- [25] A. Ferancová, S. Rengaraj, Y. Kim, J. Labuda, M. Sillanpää, Biosens. Bioelectron. 26 (2010) 314–320.
- [26] J.Z. Yang, J.W. Yu, J. Fan, D.P. Sun, W.H. Tang, X.J. Yang, J. Hazard. Mater. 189 (2011) 377–383.
- [27] T.Y. Zhai, X.S. Fang, Y. Bando, Q. Liao, X.J. Xu, H.B. Zeng, Y. Ma, J.N. Yao, D. Golberg, ACS Nano 3 (2009) 949–959.
- [28] M. Gunasekaran, M. Ichimura, Sol. Energ. Mater. Solar Cells 91 (2007) 774–778.
- [29] Z.X. Huang, F.Q. Sun, Y. Zhang, K.Y. Gu, X.Q. Zou, Y.Y. Huang, Q.S. Wu, Z.H. Zhang, J. Colloid Interface Sci. 356 (2011) 783–789.
- [30] I. Fasaki, K. Siamos, M. Arin, P. Lommens, I. Van Driessche, S.C. Hopkins, B.A. Glowacki, I. Arabatzis, Appl. Catal. A – Gen. 411–412 (2012) 60–69.
- [31] N.Z. Bao, L.M. Shen, T. Takata, D.L. Lu, K. Domen, Chem. Mater. 20 (2008) 110–117.
- [32] X. Li, J. Zhu, H.X. Li, Appl. Catal. B: Environ. 123–124 (2012) 174–181.
- [33] K. Azlan, W.N.W. Saime, L.L. Ken, J. Environ. Sci. 21 (2009) 296–302.
- [34] W.J. Li, D.Z. Li, Y.M. Lin, P.X. Wang, W. Chen, X.Z. Fu, Y. Shao, J. Phys. Chem. C 116 (2012) 3552–3560.
- [35] Y.Y. Li, J.S. Wang, H.C. Yao, L.Y. Dang, Z.J. Li, J. Mol. Catal. A: Chem. 334 (2011) 116–122.
- [36] S. Song, L.J. Xu, Z.Q. He, J.M. Chen, Environ. Sci. Technol. 41 (2007) 5846–5853.
- [37] W. Zhao, C.C. Chen, X.Z. Li, J.C. Zhao, J. Phys. Chem. B 106 (2002) 5022–5028.
- [38] L. Gomathi Devi, R. Kavitha, Appl. Catal. B: Environ. 140–141 (2013) 559–587.